# Behaviour Of Rectangular Hollow Steel Beams Strengthened With Multi-Layers Of Transversal CFRP Wrapping

Anwar Badawy Abu-Sena, Hanan Hussien Eltobgy, Omer Nazmi Abdelnabi

**Abstract**– This paper aims to study the impact of hollow steel beams reinforced by carbon fibers reinforced polymers (CFRP) applied in transversal directions. Experimental and numerical investigations were carried out in this study. This study has focused on the impact of increase the number of wrapping layers. Six specimens of rectangular hollow sectional (RHS) were included in the experimental study. Specimens were subjected to a four-point bending test and divided into two groups according to the case of applied bending moment; the First group was subjected to bending moment about the major axis while the second group was subjected to bending moments about the minor axis. The behavior and strength of specimens were determined through the experimental tests. The numerical model was developed using a finite element program in order to predict the failure load of tested beams. Results of the numerical model were verified with the corresponding results of the experimental test, and a good agreement was observed. As per experimental results, transversal wrapping systems of CFRP can delay the buckling occurrence of strengthened steel beams. Hence, it is capable of improving the strength and the deflection of strengthened beams. Also, increasing the number of CFRP wrapping layers in the strengthening system, increase the improvements compared to strengthened beams with a single layer of CFRP.

**Index Terms**: Rectangular Hollow Steel Section, CFRP, Strengthening, Stiffness, Strength, Pucks' failure criteria

## 1. INTRODUCTION

Strengthening techniques with CFRP approve a great potential to restore the strength of deteriorated structures or to improve the capacity for strengthened ones. Applications of CFRP techniques are widely utilized with various concrete and steel structures. Hollow steel sections (HSS) are commonly preferred due to aesthetic and engineering reasons. Hollow section shape provides a large rigidity and stiffness compared to other shapes. Thus, hollow steel section can minimize the cost of construction by providing the least sectional weight to endure applied loads. Which make these sections a highly susceptible to buckling phenomena and corrosion. So, CFRP wrapping techniques are very useful in the strengthening and the rehabilitation of hollow steel sections. Recently, many studies have been conducted to investigate the efficiency of CFRP techniques in the strengthening of hollow steel section. Abu-Sena et al. [1] experimentally and numerically investigated twenty hollow steel columns reinforced with CFRP techniques. The full wrapping technique for external bonding CFRP sheets provides sufficient confining action against column local deformation, which delays elastic local buckling and increases column axial capacity and stiffness. While, failure occurred at the non-strengthened zones between CFRP strips in partially strengthened specimens. SHS specimens had an increase in ultimate capacity of 19.1% to 34.5 percent, while RHS specimens had an increase of 18% to 41.3 percent. Chen et al. [2] experimentally investigated the flexural behavior of rectangular hollow section (RHS) steel beams with initial crack strengthened externally with carbon fiber reinforced polymer (CFRP) plates. Eight specimens were subjected under three-point loading test, three of beams were control specimens while rest of beams strengthened with CFRP plates with or without prestressing. Adhesive resin and two anchorage systems were proposed to reinforce bottom flange of steel beams with CFRP plates. It was observed that the techniques can significantly reduce the deformation of repaired cracked specimens, and debonding of interface between CFRP and steel is vital to the specimens under large load. Also, the prestressing CFRP plate can further increase the yield load and increase the utilization efficiency of the CFRP plate. Chahkand et al. [3] experimentally studied the behaviour of CFRP reinforced square hollow section (SHS) beams in pure torsion. Tested specimens were strengthened with several configuration of CFRP sheets; vertical, spiral, and reverse-spiral wrapping. It was found that utilizing CFRP strengthening techniques effectively improved the elastic and plastic torsional strength of strengthened specimens. The number of layers of CFRP and the strengthening configurations were important factors for the improvement. Using spirally wrap configuration is the most effective configuration at resisting applied torque where carbon fibers are oriented in the direction of the principal tensile stresses. While Keykha A.H. [4] numerically investigated CFRP strengthened deficient square hollow steel sections and subjected to combined tensile, torsional, and lateral load. It is found that CFRP techniques have an impact on improving the ultimate capacity and can significantly restore the lost strength of deficient elements. Although many of literatures have concerned of CFRP strengthening of hollow steel sections, rectangular hollow sections with highly aspect ratio have not been covered. Also, most of studied works have not included pure bending moment in their investigations. Therefore, this study attempts to fill in the gaps in this topic by studying the behaviour of rectangular hollow steel section strengthened with CFRP. Experimental and numerical investigations were performed for six specimens subjected to pure bending moments about major and minor axes. Tested specimens included two bare specimens and four strengthened specimens.


- *Professor of Steel Structures, Civil Engineering Department, Faculty of Engineering at Shoubra, Benha University, Email: A.Badawy@feng.bu.edu.eg*
- *Associate Professor of Steel Structures, Civil Engineering Department, Faculty of Engineering at Shoubra, Benha University, Email: hanan.altobgy@feng.bu.edu.eg*
- *Assistant Lecturer, Civil Engineering Department, Faculty of Engineering at Shoubra, Benha University, Cairo, Egypt, Email: omer.nazmi@feng.bu.edu.eg*

## 2. EXPERIMENTAL PROGRAM

### 2.1 Specimen dimensions

Experimental program was prepared to evaluate the influence of using carbon reinforced fiber polymer sheets in the strengthening of highly aspect ratio of rectangular hollow steel section. Table 1 shows the variable dimensions of experimental program. Six specimens divided in two groups were selected. Group G1 and G2 were subjected to bending moment about major axis and minor axis, respectively. Each group consists of three specimens different on strengthening case and/or wrapping technique. Steel section size 150*50*1.8 was selected with deep web plate in order to investigate the CFRP effects on the buckling failure modes. Slender status of sectional plates were determined according to width to thickness ratios limits presented at table 4.1b, AISC360-16 [6] using averaged yield stresses resulted from the coupon tests conducted in this study. Figure 1 shows schematic for transversally CFRP wrapping techniques applied on tested specimens. Two wrapping techniques of CFRP sheets were utilized in this study. Term “FRP -1T” refers to steel specimen wrapped with a single layer of CFRP applied on transversal direction. Term “FRP -1T 2T” refers to steel specimen wrapped with a double layers of CFRP applied on transversal direction. While term “NOFRP” refers to control specimen without any wrapping.

### 2.2 Material properties

Four coupons were prepared where width and length of reduced section are 20mm, 80mm respectively. Figure 2 shows the determined stress-elongation diagrams of tensile coupon tests. Mechanical properties of steel material were determined from the results of tensile coupon tests, average yield and average ultimate stresses are 322Mpa and 374Mpa, respectively. For CFRP strengthening system, a composite systems consisted of unidirectional carbon fiber fabrics “SikaWrap-230C” and adhesive resin “Sika dur ®-330” were utilized, [7 and 8]. Figure 3 shows the roll of utilized unidirectional carbon fiber sheets, SikaWrap®-230C and a close view of woven fabrics.

### 2.3 Specimen Preparation

Steel surface shall be clean, dry, and free of rusts and other contaminants such as dust, foreign particles, oil, grease, and surface coatings, among others, that could disrupt or prevent the adhesion of the composite strengthening system with steel surface. Mechanical processing with a rotary wire brush and sandpapers, as well as a chemical cleaning with a thinner-based solvent, were utilized to prepare the surface of steel specimens well for applying the CFRP laminate. Two-component epoxy resin, Sikadur®-330 is used for the priming coat and as the impregnating material in the dry application of the SikaWrap®-230C system. According to the manufacturer guidelines, two components of the resin were mixed and applied to the prepared steel surfaces. Right after that, carbon fiber fabrics were wrapped all over the adhesive film in the orientation required for each specimen. Then, all specimens were left for two weeks to produce an excellent connection between steel and CFRP, [7 and 8]. Figure 4 shows sample of steel specimens during preparing the adhesive resin coat for CFRP application. Figure 4. Show sample of prepared specimens after applying wrapping system and fixing strain gages. All specimens have a total length 2000mm where wrapping sheets covered 1600mm mediate the length of strengthened steel beam. Also, strain gauges were installed over CFRP laminates at the middle of the beam aligned with longitudinal fiber direction. Strain gages were fastened at the bottom flanges in case of longitudinal layers and fastened at the top flanges in case of transversal layers.

***TABLE 1. SPECIMENS PROPERTIES.***

| Group no. | Section size Depth* Width*Th. | Aspect ratio | Slenderness ratio | | Specimens ID |
|---|---|---|---|---|---|
| | d * b * t | b/d | d/t | b/t | |
| G1 | RHS 150*50*1.8 | 1/3 | 80.3 (N.C.) | 24.7 (C.) | B11-150-50-NOFRP |
| | | | | | B13-150-50-FRP-1T |
| | | | | | B15-150-50-FRP-1T 2T |
| G2 | RHS 50*150*1.8 | 3 | 24.7 (C.) | 80.3 (S.) | B16-50-150-NOFRP |
| | | | | | B18-50-150-FRP-1T |
| | | | | | B20-50-150-FRP-1T 2T |

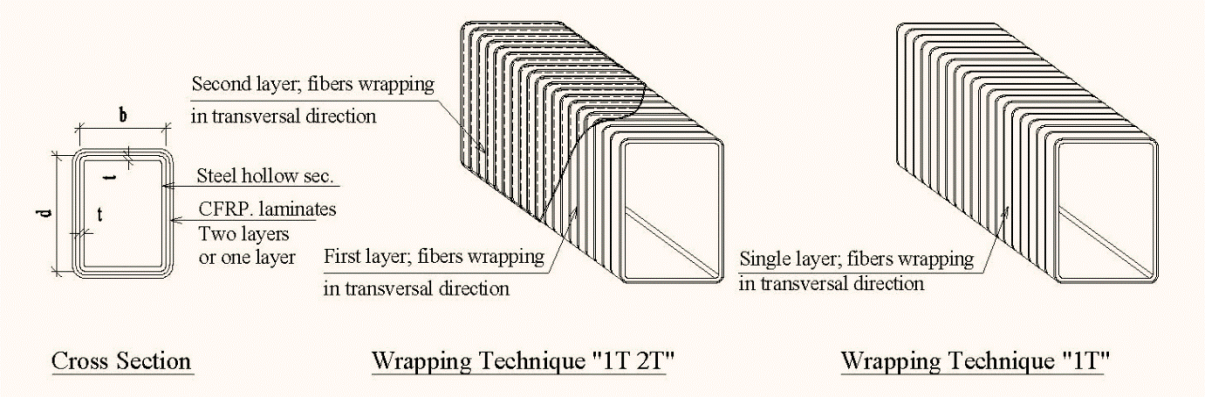


***FIGURE 1.*** *SCHEMATIC VIEW FOR STRENGTHENING TECHNIQUES, 1T2T & 1T.*

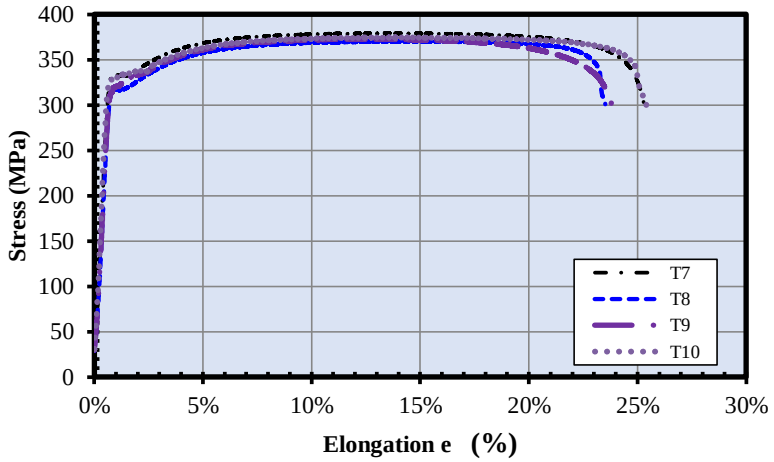


***FIGURE 2.*** *STRESS-ELONGATION DIAGRAMS OF COUPON TESTS.*

A) CARBON FIBERS FABRIC ROLL

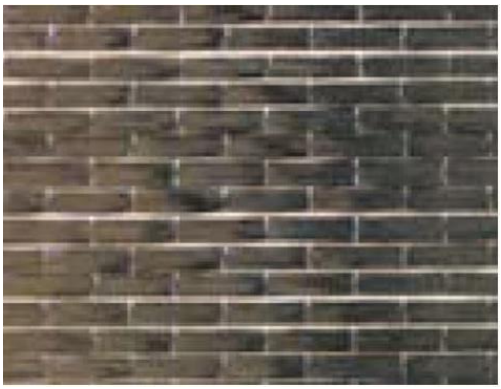

B) CLOSE VIEW OF UNIDIRECTIONAL FABRIC

***FIGURE 3 .*** *UNIDIRECTIONAL CARBON FIBER SHEETS, SIKAWRAP-230C*

***FIGURE 4.*** *MIXING AND APPLYING OF ADHESIVE RESIN ON STEEL SURFACE.*

***FIGURE 5.*** *SAMPLES OF PREPARED SPECIMENS AFTER WRAPPING AND FIXING STRAIN GAGES.*

### 2.4 Testing method

Figure 6 shows the test setup used with specimens B20-1T 2T as an example of performed tests, and shows the various utilized instruments, spreader beam, LVDT, loading cell, and hydraulic jack. All specimens were subjected to four-point bending tests with clear span 1900mm. Experiments were carried out using a hydraulic jack, a hydraulic pump, and a 500 KN loading cell. The imposed load was transferred in two independent positions over the specimen using a spreader beam. Internally induced pure bending moment in the central region of the beam. To eliminate stress concentrations, specimens were also furnished with bearing plates and stiffener plates. Linear voltage displacement transducers (LVDT) were also employed to determine beam deflections at three points: the middle of the beam, and the application of loads. Several measurements were collected from attached instruments, loading cell, LVDTs, and strain gauges during the testing procedure by the Data logger system. Vertical load was applied to specimens in incremental steps until failure occurred. For each specimen, failure mode shape associated with ultimate load was also observed.

### 2.5 Experimental results and discussion

The ultimate applied load and relative deflection for all tested specimens are presented in table 2. Specimen's deflections relative to ultimate loads of corresponding bare beam are presented as well. When compared to the results of bare steel beams, the ultimate load and deflection of strengthened specimens were much higher. For specimens B13-1T, B15-1T 2T, B18-1T, and B20-1T 2T, the improvement percentage of ultimate loads is 14 percent, 20 percent, 17 percent, and 24 percent, respectively, while the improvement percentage of corresponding deflections is 23 percent, 19 percent, 23 percent, and 29 percent.

**Ultimate loads and deflections.**

Figures 7. a and b present vertical load –deflection curves of the tested specimens of group G1 and G2, respectively. The plotted curves show the behavior of strengthened and reference specimens during experimental tests. One can see that while ultimate loads approach, all curves tend to decrease, signifying that buckling happens, causing a reduction in beam stiffness. The curve declination of the CFRP strengthened beam, on the other hand, was less significant. This is due to the CFRP wrapping, which was efficient in constraining buckling deformations and therefore boosting strength.

**Ultimate loads and Failure modes**

Figures 16 and 17 show the failure mode for specimens, B20-1T2T and B11-NOFRP, respectively. It can be noticed the occurrence of web crippling phenomena at the loading regions associated with flexural failure mode of specimen, B11-NOFRP as an example of specimens' group G1. While, flange buckling mode can be noticed with specimen B20-1T2T as an example of specimens' group G2, which referred to the wide flange plate with high susceptibility for buckling. Physical defects to CFRP laminates were also detected at loaded zones, which contributed to the overall failure mode. Furthermore, during all specimen testing, no slippage failure between CFRP sheets and steel surfaces was found.

***Table 2. Experimental results: ultimate loads and deflections.***

| Assembly no. | Specimens ID | Ultimate load (kN.) | Ultimate load ratio | Deflection at failure (mm) | Corresponding deflection (mm) | Corresponding deflection ratio |
|---|---|---|---|---|---|---|
| G1 | B11-150-50-NOFRP | 24.08 | 1.00 | 11.35 | 11.35 | 1.00 |
| | B13-150-50-FRP-1T | 27.39 | 1.14 | 10.57 | 8.70 | 0.77 |
| | B15-150-50-FRP-1T 2T | 28.93 | 1.20 | 13.83 | 9.16 | 0.81 |
| G2 | B16-50-150-NOFRP | 8.35 | 1.00 | 21.80 | 21.80 | 1.00 |
| | B18-50-150-FRP-1T | 9.75 | 1.17 | 25.80 | 16.86 | 0.77 |
| | B20-50-150-FRP-1T 2T | 10.34 | 1.24 | 28.30 | 15.50 | 0.71 |

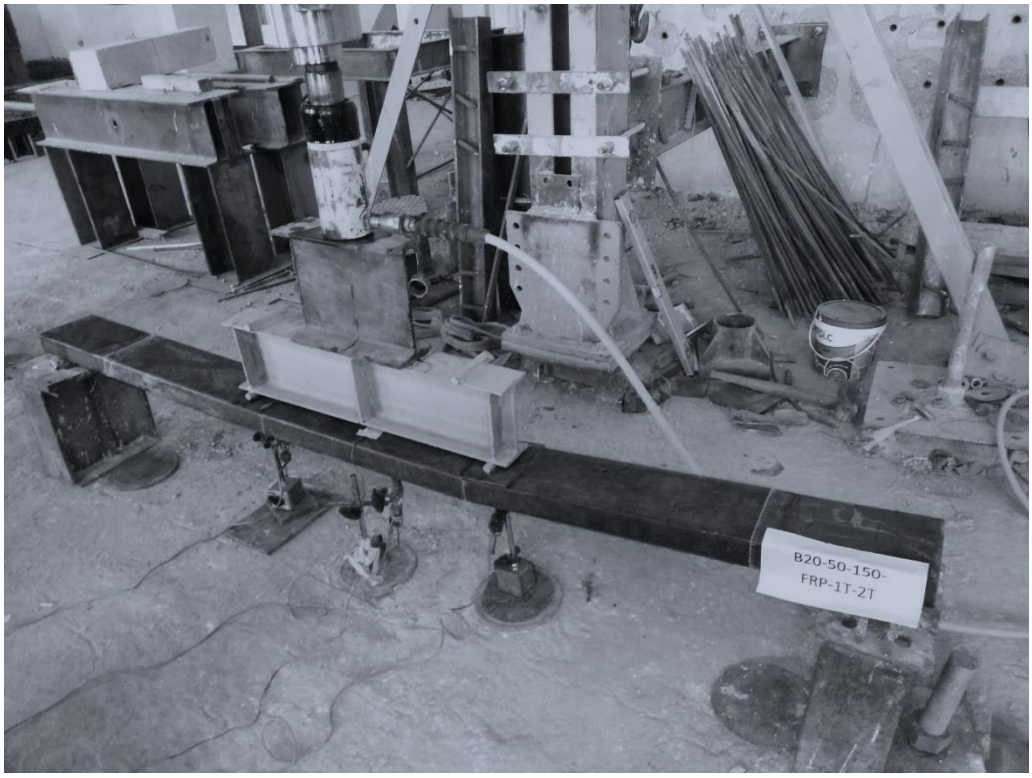


***FIGURE 6** CONFIGURATION OF BENDING TEST FOR SPECIMEN B20-1T 2T., AS AN EXAMPLE*

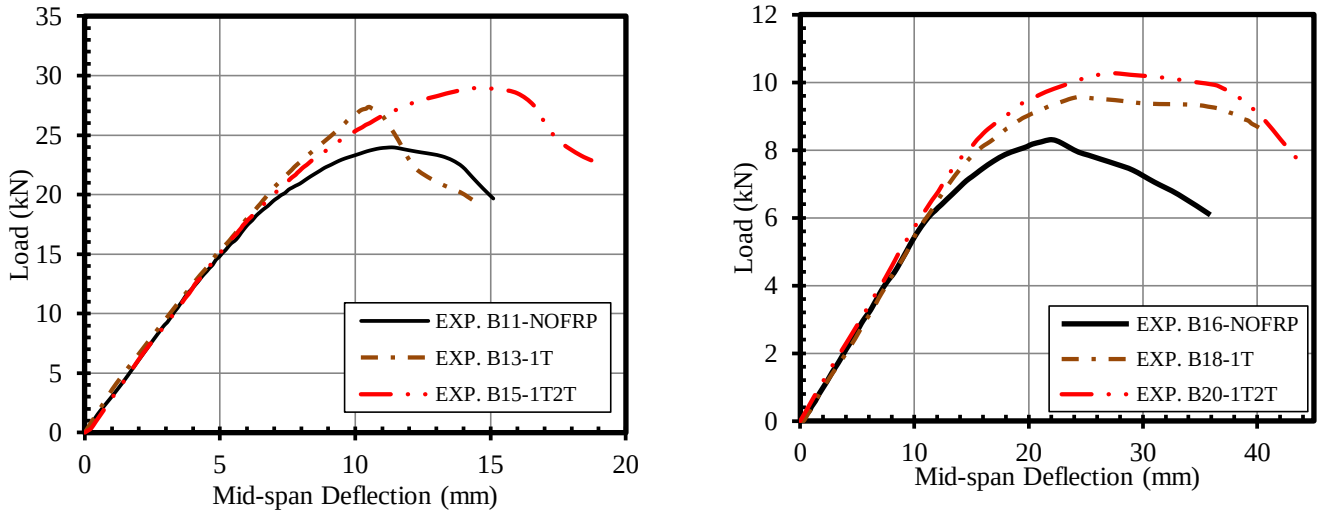


a.) For specimens' group G1

b.) For specimens' group G2

***Figure 7*** *load versus mid-span deflection curves.*

**Ultimate Loads and Strain**

Figures 8 displays the recorded CFRP laminate strains versus applied loads for groups G1 and G2. It can be noticed that all recorded strains do not reach the ultimate laminate elongation "0.0156" provided by the manufacturer data sheet. The recorded strains show the role of CFRP laminates in delaying the failure mode of flange local buckling or flange yielding.

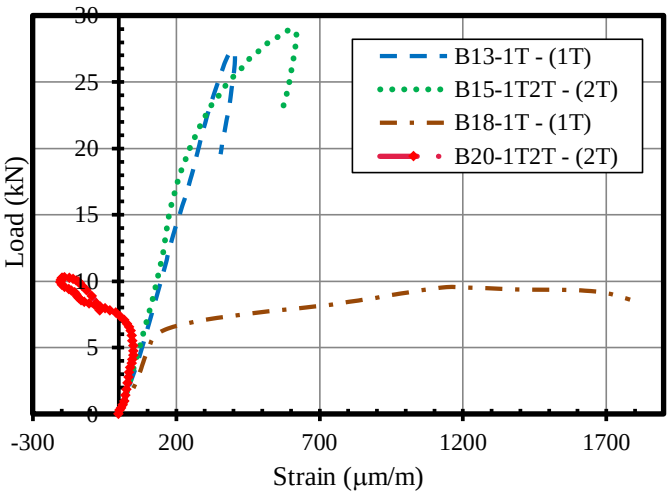


***FIGURE 8.*** *LOAD – STRAIN DIAGRAMS*

## 3. Finite element analysis (FEA) model

ANSYS 17.2 [9], a commercial tool, was used to simulate the tested specimens. The behaviour of CFRP strengthened Rectangular hollow steel sections subjected to uniform bending moment was investigated using a finite element model. The finite element model included eigenvalue and non-linear analysis. The outcomes of the finite element analysis were compared to the experimental results in order to ensure that the developed model was reliable. Finite elements models were developed according to the condition of experimental test presented at table 1.

### 3.1 Material Modeling

Figure 9 shows the idealized stress-strain curve cold formed steel model proposed by Abdel-Rahman and Sivakumaran [10]. The idealized curve was adopted in the simulation of steel material in the analysis model. Averaged yield and ultimate stresses obtained from coupon test were utilized to produce the idealized curve for steel material. Steel was simulated in the finite element model as a multi-linear isotropic hardening material, while young's modulus (E) and Poisson's ratio (□□) were 205,000 Mpa and 0.3 respectively.

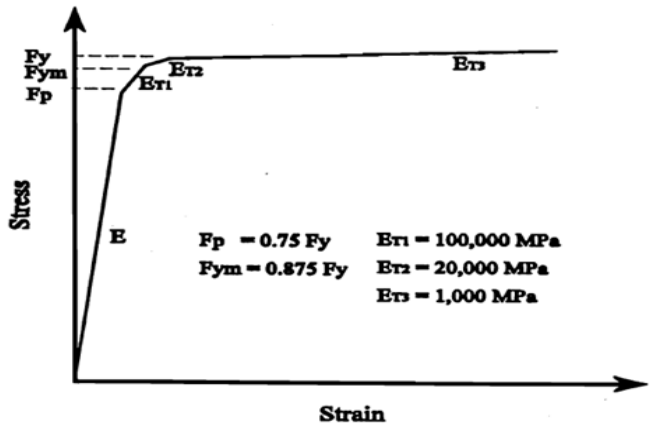


***FIGURE 9.*** *IDEALIZED STRESS-STRAIN CURVES FOR COLD FORMED STEEL, [10].*

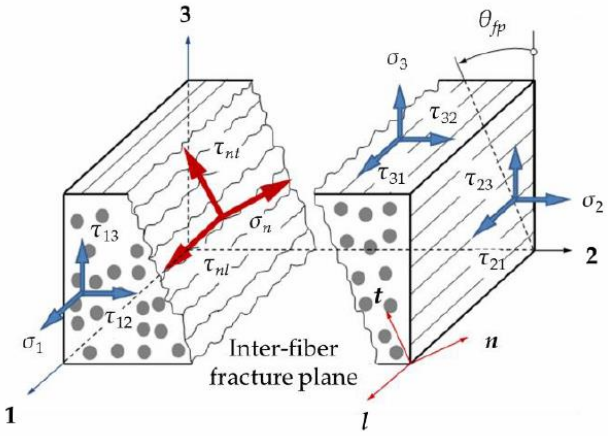


***FIGURE 10.*** *DEFINITION OF LOCAL COORDINATE SYSTEMS FOR UNIDIRECTIONAL CFRP MATERIAL 1,2,3 AND FRACTURE PLANES N, NL, NT, Jiefei Gu et al. [5].*

CFRP composite is made up of unidirectional carbon fibers that have been saturated with polymers. Carbon fibers have a superior stiffness and strength than polymers when compared to them. As a result, each design has its own set of characteristics, and CFRP composite behaves like an orthotropic material. While transversal planes perpendicular to the longitudinal direction of fibers have almost equal properties, CFRP composite can be thought of as a special case of orthotropic material known as transversally isotropic. For the simulation of CFRP laminate, Batuwitage et al. [11] used composite characteristics of carbon fibers and adhesive resin. The mechanical parameters defined in Table 3 were used to simulate CFRP laminate as a transversal isotropic linear elastic material. The mechanical properties of CFRP composite are based on laminate thickness, 0.7mm equal to effective thickness of primer resin coat ranged between 0.6mm and 0.8mm. As shown in figure 10, (1) direction is the longitudinal fibers direction, while (2) & (3) directions are the transversal fibers directions. Properties in the longitudinal direction are based on technical information about CFRP laminates found in Sika Wrap ®-230C manufacturer data sheets, [7] and were predetermined to account for the varied thickness of nominal dry carbon fibers and effective primer coat. According to research findings published by Mostofinejad et al. [12] and practical ratios presented by ECP 208 [13], compressive strength in the x-direction should be equivalent to 78 percent of tensile strength. Properties in the transversal directions are based on adhesive resin technical information found in Sika dur ®-330 manufacturer data sheets [8]. According to the research conclusions reported by Xia et al. [14] and Fernando et al. [16], shear strengths should be equal to 80% of tensile resin strength. While shear modulus was calculate using shear modulus equations presented at Kachlakev et al. [15]. As result of practical observation for the quality of applying second layer, tensile and shear strengths of second layers adopted in the analysis model were reduced by 20%.

*Table 3; CFRP Composite Properties, th. = 0.7mm.*

| Elastic modulus (Mpa) | Major Passion's ratio * | Shear modulus (Mpa) |
|---|---|---|
| $E_1$=38700, $E_2 = E_3$ = 3489 | $\nu_{23}$ = 0.3, $\nu_{12} = \nu_{13}$ = 0.22 | $G_{23}$ = 1340, $G_{12} = G_{13}$ = 2280 |
| Laminate strength (Mpa) | Matrix strength (Mpa) | Shear strength (Mpa) |
| $\sigma^f_{1t}$ = 589, $\sigma^f_{1c}$ = 459 | $\sigma^f_{2t} = \sigma^f_{3t}$ =33, $\sigma^f_{2c} = \sigma^f_{3c}$ =81 | $\sigma^f_{23} = \sigma^f_{12} = \sigma^f_{13}$ =26 |

** Poisson's ratio were taken from a similar products presented by Kachlakev et al. [15].*

Pucks' failure criteria [17 and 21] and a progressive damage model were used to simulate CFRP laminate post-failure behaviour in this investigation. Pucks' failure criteria are used to determine when a CFRP composite will fail. It has well-defined criteria for analyzing fiber and inter-fiber failure modes [18], as well as a high level of accuracy when compared to other methods [19]. Inter-fiber failure (IFF) modes can be thought of as the highest stresses coming from the critical orientation angle of the fracture planes, as shown in figure 7. Whereas, the progressive damage model is capable of modelling the post-failure behaviour of CFRP laminate by instantly reducing material stiffness after failure. ANSYS program are used to define Pucks' failure criteria. When one of the criteria parameters exceeds unity, failure occurs instantly. Axial and shear strengths and inclination parameters for IFF failure envelopes have to be defined to determine Pucks' criteria parameters. Axial and shear strengths were defined by presented data in table 3. While inclination parameters were defined using recommended values for CFRP $P^t_{xz}$ = 0.35, $P^c_{xz}$ = 0.20, $P^t_{yz} = P^c_{yz}$ = 0.27 , puck et al. [17].

### 3.2 Element Types and Mesh

The two-dimensional shell element "Shell 181" was used to simulate test specimens as a three-dimensional finite element model [20]. Shell 181 is a four-node shell element, each with six degrees of freedom, as shown in figure 11. "Shell 181" can describe plasticity, great deflections, and large strains. To achieve sufficient accuracy, fine mesh was used in the plate modelling.

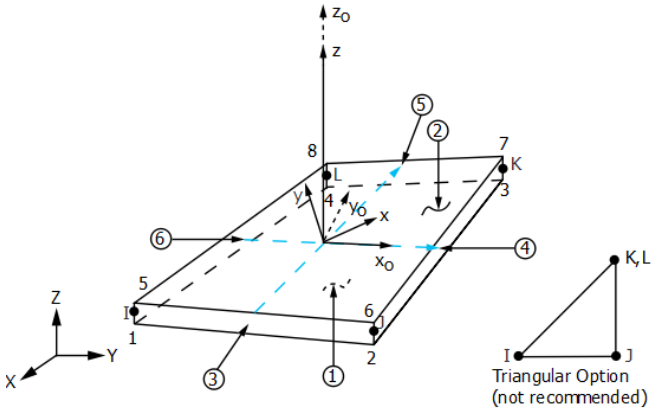


$x_o$ = Element x-axis if ESYS is not provided.

x = Element x-axis if ESYS is provided.

***FIGURE 11*** *SHELL 181 INPUT DATA, [9].*

In addition, the shell section of "Shell 181" can be defined as multilayer, with variable characteristics defining each layer. Figure 12 illustrates layers arrangements, layers numbers and layers orientations for CFRP laminates reinforced steel plates which were varied according adopted wrapping techniques.

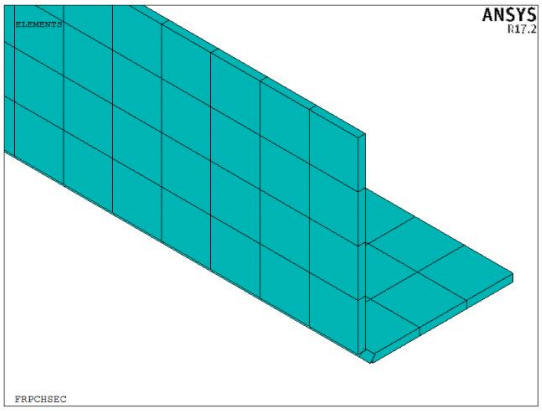


*1.A.) EXTRUDED PART VIEW FOR UNSTRENGTHEN SHELL ELEMENTS DEFINED USING SINGLE LAYER (STEEL).*

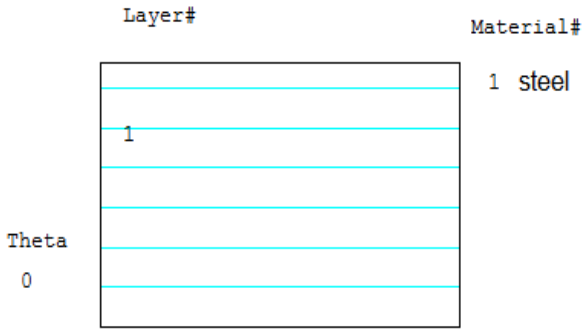


*1.B.) ORIENTATION DEFINITION FOR SINGLE LAYER FOR STEEL PLATES WITHOUT ANY WRAPPING.*

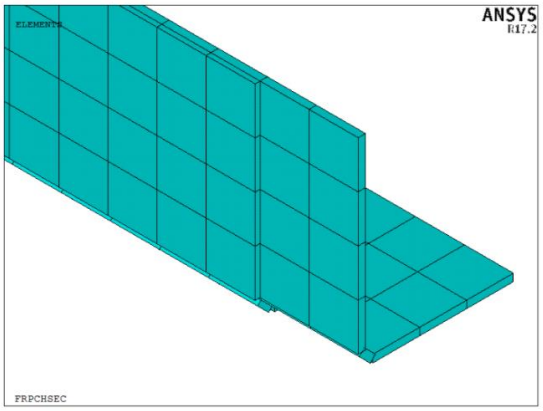


*2.A.) EXTRUDED PART VIEW FOR STRENGTHEN SHELL ELEMENTS DEFINED USING TWO LAYERS (STEEL &1T).*

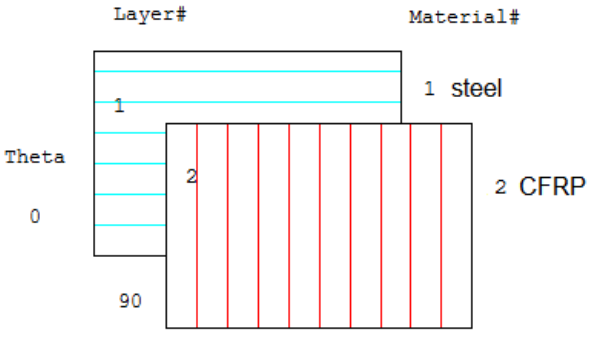


*2.B.) ORIENTATION DEFINITION STEEL LAYER FOLLOWED BY CFRP LAYER (1T).*

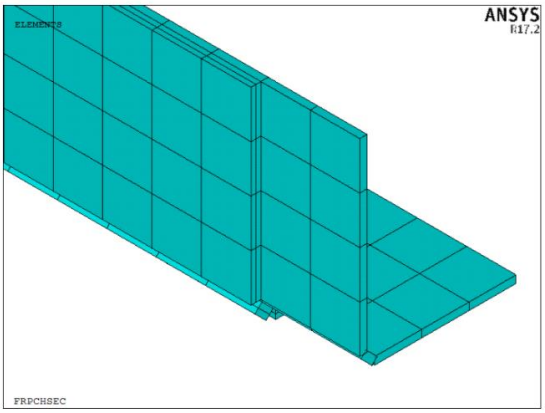


*3.A.) EXTRUDED PART VIEW FOR STRENGTHEN SHELL ELEMENTS DEFINED USING THREE LAYERS (STEEL & 1T 2T).*

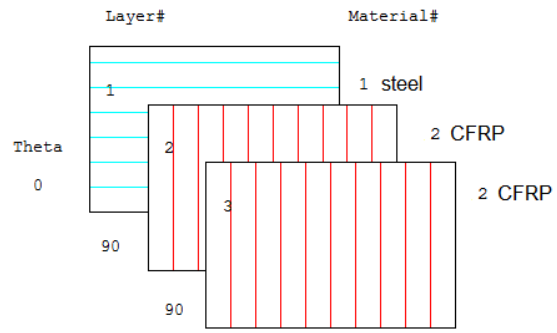


*3.B.) ORIENTATION DEFINITION STEEL LAYER FOLLOWED BY TWO CFRP LAYER (1T 2T).*

***FIGURE 12.** SHELL DEFINITIONS AT FINITE ANALYSIS MODEL; LAYERS NUMBERS, LAYERS ORIENTATIONS AND MATERIAL MODEL.*

### 3.3 Boundary Conditions

Finite model was established as a simply supported beam matching to preformed tests. Lower nodes were constrained against vertical, longitudinal, and lateral translation at hinged support. Lower nodes were constrained against translation in vertical and lateral directions at roller support. The boundary conditions of both ends are depicted in Figures 13.a and 13.b. As illustrated in Figures 13.c, the test load was simulated as nodal loads assigned to the top flange nodes specified by the loading plate region. The deferential stiffness between nodes across the beam flanges was the first reason why sides' flanged nodes were exclusively used for loading applications. The second reason is web cribbing at loading zones, which prompted flanges to lose direct contact with the loading plates.

### 3.4 Analyses Types

Eigenvalue analysis and nonlinear analyses were used in this work. Eigen value analysis was employed to get the buckling shape of the critical mode, which was subsequently scaled to imitate the initial geometrical defect. According to measured dimensions for steel sections, the maximum observed bows for groups G1 and G2 related to sectional depth are 0.75mm. Using the measured values, the maximum amplitude of the initial defect was determined. As an example, Figure 14 shows the critical buckling mode form for RHS 150*50*1.8. The local buckling of section plates was related with the first buckling mode. Nonlinear material, progressive damage evolution, and large displacement were used in the finite element model. Analyses were carried out using the arc-length method as an incremental load control to determine collapse loads.

### 3.4 Finite Element Validation

The finite element models were validated against the experimental testing using load displacement curves, failure mode shapes, and ultimate loads. The load-deflection curves developed from finite element analysis and those obtained from experimental tests are shown in Figure 15. The results are in good agreement, as shown by the curves. Table 4 compares the ultimate vertical loads and related deflections obtained from experimental tests and finite element modelling for each specimen. Good agreement can be observed between them, where the ratio of experimental to finite element ultimate loads for all specimens ranges between 0.96 and 1.02, and the mean value and coefficient of variation are 0.98 and 0.026, respectively.

Figures 16 and 17 compares between the deformed shapes and failures modes obtained from the finite element analysis and the experimental tests for specimens B20-1L2T and B11-NOFRP, respectively. Internal steel stress was plotted on the deformed shape of finite element model which indicates that reaching the failure was combined by buckling occurrence. Also, failed regions of CFRP laminates 1T and 2T predicted by Puck's failure criteria and degradation model are shown in figures 16. e to h aside with the experimental test. Comparisons show a good similarity between relative deformed shapes and failures modes. Also, failed regions of CFRP laminates predicted by finite element model are in a good agreements with physical damaged regions observed in experimental tests. According to the comparative results, the developed F.E. model could be used to estimate the performance and strength of steel hollow beams reinforced with CFRP.

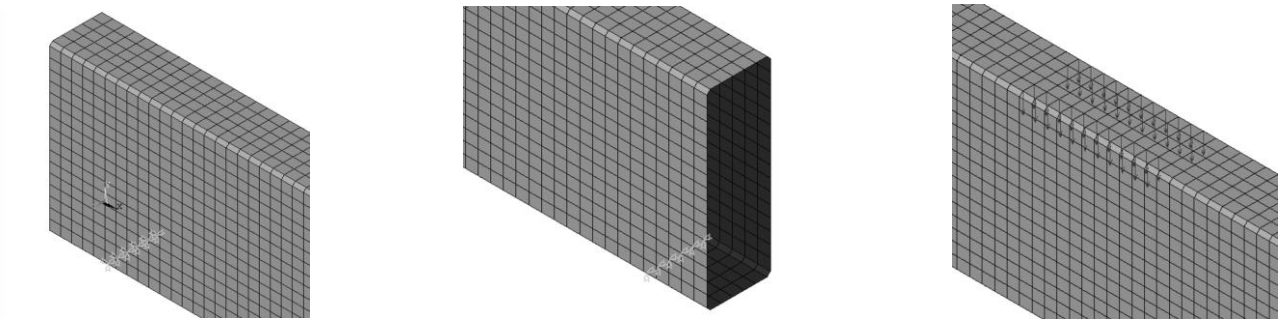

A.) FOR HINGED SUPPORT. B.) FOR ROLLER SUPPORT C.) LOAD APPLICATION.

***FIGURE 13.*** *BOUNDARY CONDITIONS AND LOADS*

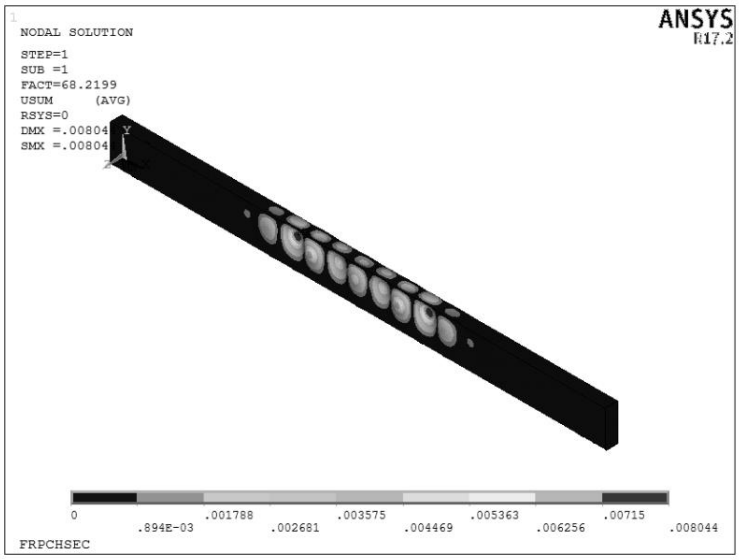


***FIGURE 14.*** *CRITICAL MODE SHAPE FOR SHS 100*1.5 AS AN EXAMPLE.*

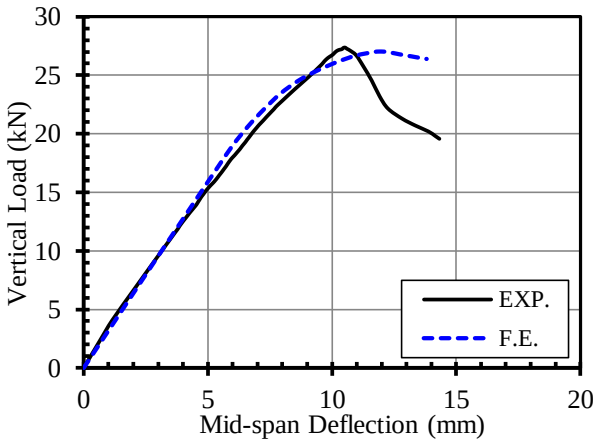


*Specimen B13*

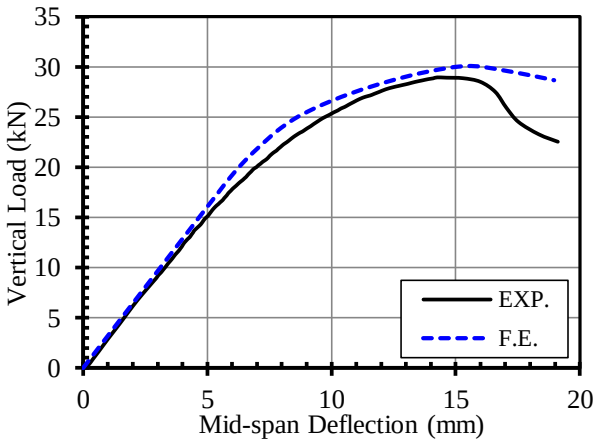


*Specimen B15*

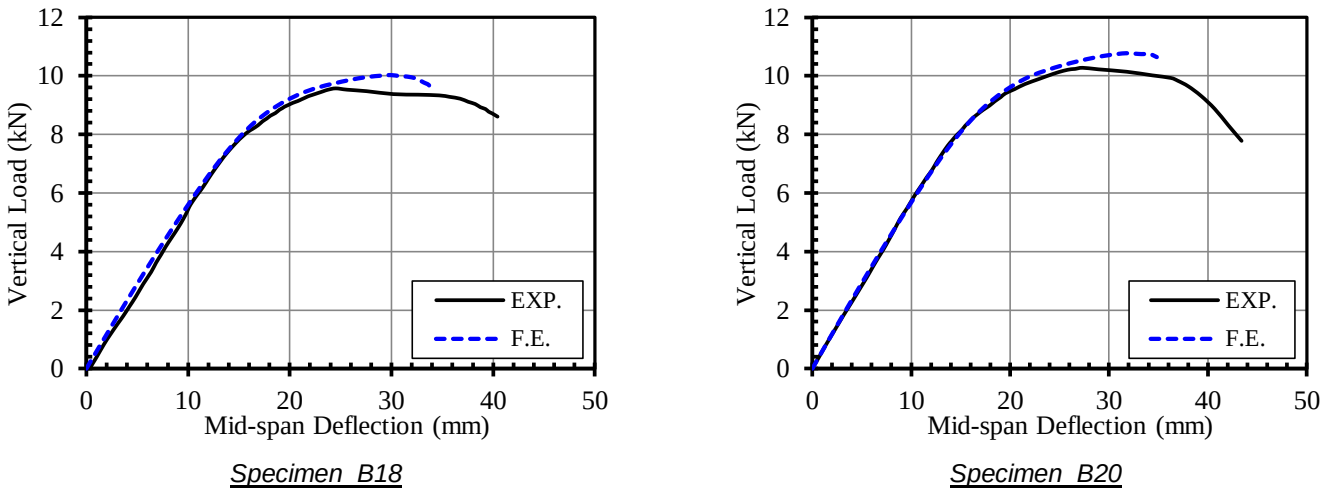


***FIGURE 15.*** *VERTICAL LOAD – MID-SPAN DEFLECTION CURVES OF STRENGTHENED SPECIMENS*

***TABLE 4. COMPARISON BETWEEN EXPERIMENTAL AND FINITE ELEMENT ULTIMATE CAPACITIES***

| Group no. | Specimens ID. | Ultimate load (kN.) | | | Deflection at ultimate load (mm) | | |
|---|---|---|---|---|---|---|---|
| | | Exp. | F.E. | Exp. / F.E. | Exp. | F.E. | Exp. / F.E. |
| G1 | B11-150-50-NOFRP | 24.08 | 23.65 | 1.02 | 11.35 | 8.80 | 1.29 |
| | B13-150-50-FRP-1T | 27.39 | 27.00 | 1.01 | 10.57 | 11.90 | 0.89 |
| | B15-150-50-FRP-1T 2T | 28.93 | 30.06 | 0.96 | 13.83 | 15.50 | 0.89 |
| G2 | B16-50-150-NOFRP | 8.35 | 8.54 | 0.98 | 21.80 | 22.30 | 0.98 |
| | B18-50-150-FRP-1T | 9.75 | 10.06 | 0.97 | 25.80 | 31.12 | 0.86 |
| | B20-50-150-FRP-1T 2T | 10.34 | 10.77 | 0.96 | 28.30 | 31.70 | 0.89 |
| Mean value (μ) | | | | 0.98 | | | 0.966 |
| Standard deviation (S) | | | | 0.025 | | | 0.163 |
| Coefficient of variation (V) = S / μ | | | | 0.026 | | | 0.169 |

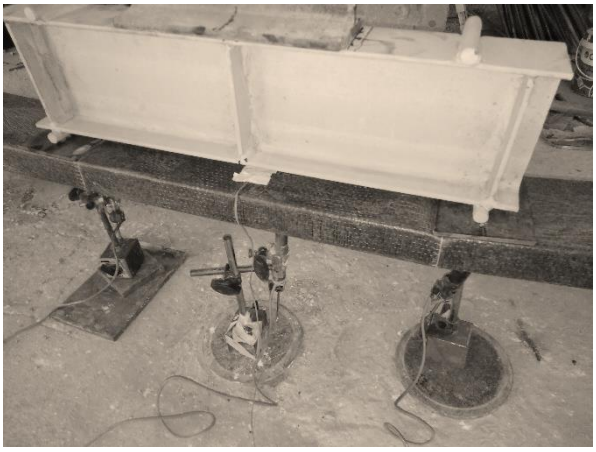

*A.) EXPERIMENTAL FAILURE MODE.*

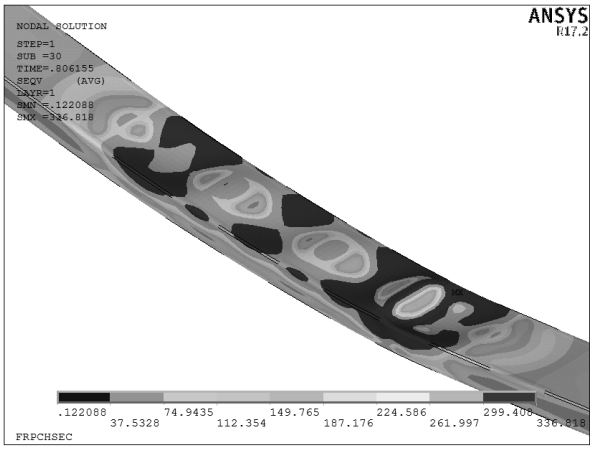


*B.) F.E. DEFORMED SHAPE WITH CONTOURED STEEL STRESSES.*

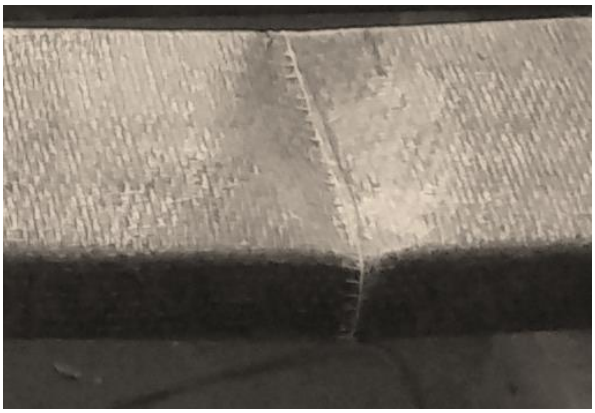

c.) *Experimental buckling at loading region.*

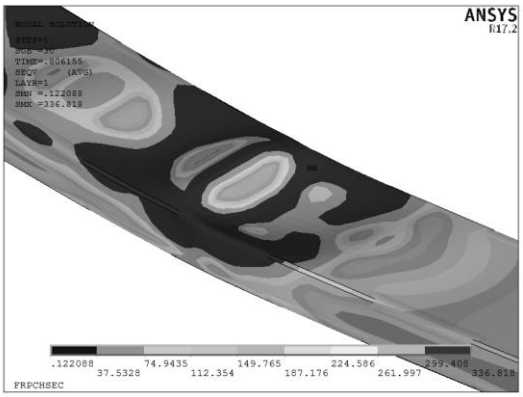


d.) *F.E. yielding stress at loading region.*

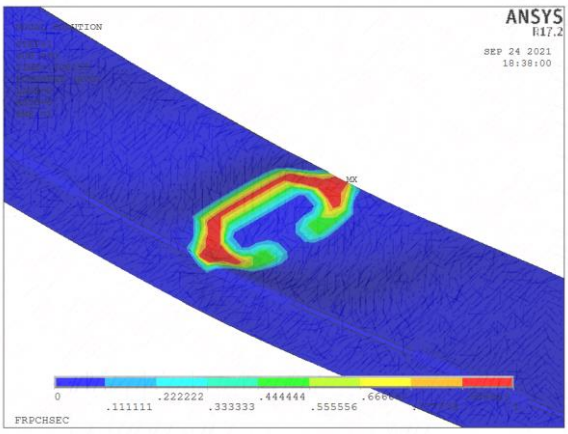


e.) *Contoured degradation of failed CFRP laminate,1T*

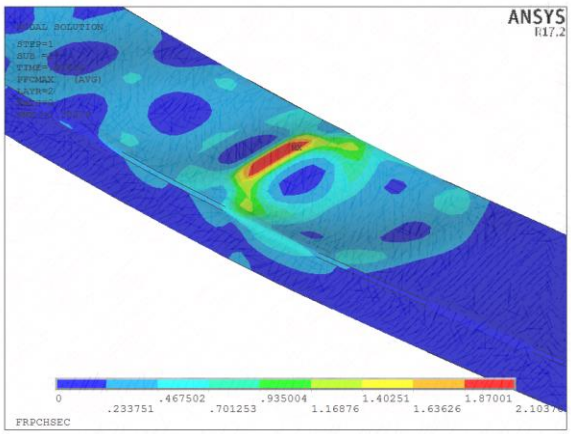


f.) *Contoured Puck's stress factor of CFRP laminate, 1T.*

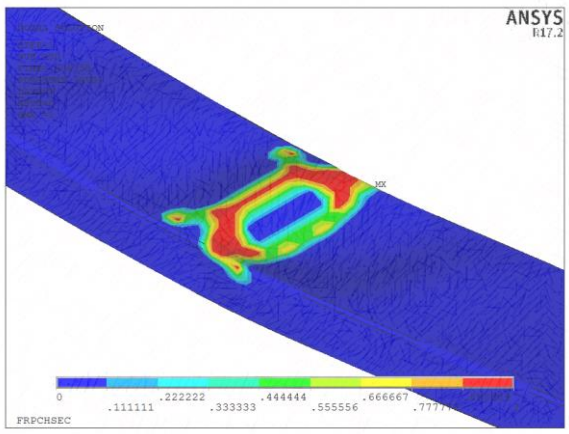


g.) *Contoured degradation of failed CFRP laminate,2T*

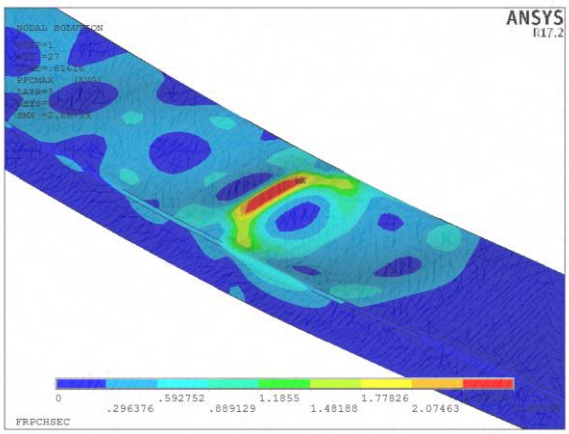


h.) *Contoured Puck's stress factor of CFRP laminate, 2T.*

***Figure 16.*** *Comparison between deformed shapes of specimen, B20-1T 2T obtained from tests and F.E.*

*A.) EXPERIMENTAL FAILURE MODE.*

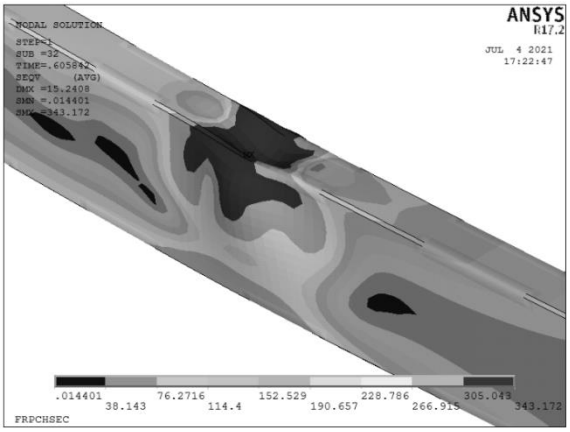


*B.) F.E. DEFORMED SHAPE WITH CONTOURED STEEL STRESSES.*

***FIGURE 17.*** *COMPARISON BETWEEN DEFORMED SHAPES OF SPECIMEN, B11-NOFRP OBTAINED FROM TESTS AND F.E.*

## 4. CONCLUSIONS

This paper experimentally and numerically investigated the structural performance of RHS strengthened by one layer and two layers of transversal CFRP laminates. Adopting the configuration of four-points loading test, six specimens divided in two groups were subjected to bending moments about the major and the minor axes divided in two similar group. Using the ANSYS tool, a finite element model was created to simulate CFRP strengthened beams. To imitate the failure behaviour of CFRP laminate, Puck's failure criterion and a progressive damaged model were used. The experimental results corroborated the results of the F.E. model. According to the findings of the experiments, all reinforced specimens outperformed control specimens in terms of strength. The following are the key conclusions of this study; The model was created with the help of a finite element program. ANSYS properly simulates and predicts the behaviour of CFRP-strengthened hollow steel beams, including loads and deflection. Regardless of the loading axis, all CFRP wrapping procedures significantly improved the ultimate capacity and deflection of rectangular hollow steel sections subjected to four point loading tests when compared to the results of bare steel beams. Steel section buckling plays a significant effect in the strength enhancement ratios achieved by strengthening hollow steel beams with CFRP wrapping techniques. Transversal wrappings could confront the deformations resulted from web crippling phenomena or flange local buckling and delay buckling occurrence. Thus, increase the strength of strengthened beams. With all strengthened specimens, the use of a double layer of transversal wrapping technique called "1T 2T" resulted in a significant increase in ultimate load and deflection. So, Greater gains can be made by increasing the number of transversal layers as long as steel sections are prone to local buckling events.

## References

[1]. Abu-Sena A.A.B, Said M, Zaki M.A, and Dokmak M. “Behavior of Hollow Steel Sections Strengthened with CFRP” Construction and Building Materials, 205 (2019) 306–320

[2]. Chen T, Qi M, Gu X.-L, and Yu Q.-Q. “Flexural Strength of Carbon Fiber Reinforced Polymer Repaired Cracked Rectangular Hollow Section Steel Beams” International Journal of Polymer Science Volume 2015, Article ID 204861, 9 pages.

[3]. Chahkand N. A, Jumaat M. Z, Sulong N.H.R, Zhao X.L., Mohammadizadeh M. R. “ Experimental and theoretical investigation on torsional behaviour of CFRP strengthened square hollow steel section” Thin-Walled Structures 68 (2013) 135–140

[4]. Keykha A.H, “Structural performance evaluation of deficient steel members strengthened using CFRP under combined tensile, torsional and lateral loading” Journal of Building Engineering 24 (2019) 100746

[5]. Jiefei Gu, Ke Li, and Lei Su “A Continuum Damage Model for Intralaminar Progressive Failure Analysis of CFRP Laminates” Materials 2019, 12, 3292

[6]. American Institute of Steel Construction (AISC). Manual of Steel Construction. Chicago, Illinois, USA: Load and Resistance Factor Design (LRFD); March 2016

[7]. SIKA EGYPT Company ‘‘Sika Wrap®-230C. Product data sheet” March 2020, Version 01.03.

[8]. SIKA EGYPT Company ‘‘Sika dur®-330. Product data sheet” August 2018, Version 01.01.

[9]. ANSYS, Finite Element Analysis Program and Theory Manuals, Release V17.2, 2016.

[10]. Abdel-Rahman N, and Sivakumaran K.S. “Evaluation and Modeling of the Material Properties for Analysis of Cold-Formed Steel Sections” International Specialty Conference on Cold-Formed Steel Structures. Paper 3, October 17, 1996.

[11]. Batuwitage C, Fawzia S, Thambiratnam DP, Tafsirojjaman T, Al-Mahaidi R, and Elchalakani M. “CFRP-Wrapped Hollow Steel Tubes Under Axial Impact Loading.” Tubular. Struct. XVI Proc. 16th Int. Symp. Tubular. Struct. (ISTS 2017, 4-6 December 2017, Melbourne, Aust., CRC Press; 2017, p. 401-407.

[12]. Mostofinejad D, and Moshiri N. “Compressive strength of CFRP composites used for strengthening of RC columns: comparative evaluation of EBR and grooving methods.” J. Compos. Constr. 2015; 19 (5).

[13]. ECP Committee 208-05 “Egyptian code of practice for the use of fiber reinforced polymer in the construction field” ECP Committee 208, Ministry of Housing and Urban Communities, Egypt, 2005.

[14]. Xia S.H, and Teng J.G. “Behaviour of FRP-to-Steel Bonded Joints” the International Symposium on Bond Behaviour of FRP in Structures (BBFS 2005).

[15]. Kachlakev D, Miller T, Yim S, Chansawat K, and Potisuk T. “Finite element modeling of reinforced concrete structures strengthened with FRP laminates”. Final Report SPR-316, Oregon Department of Transportation, May 2001.

[16]. Fernando D, Yu T, and Teng T.G. “Behavior and Modeling of CFRP-Strengthened Rectangular Steel Tubes Subjected to a Transverse End Bearing Load” International Journal of Structural Stability and Dynamics Vol. 15, No. 8 (2015) 1540031 (24 pages).

[17]. Puck A, Kopp J, and Knops M. “Guidelines for the Determination of the Parameters in Puck’s Action Plane Strength Criterion” Composites Science and Technology. Vol. 62.371-378. 2002.

[18]. Ozyildiz M, Muyan C, and Coker D. “Strength Analysis of a Composite Turbine Blade Using Puck Failure Criteria” 2018 J. Phys.: Conf. Ser. 1037 042027.

[19]. Dávila C.G, and Camanho P.P. “Failure Criteria for FRP Laminates in Plane Stress” NASA/TM-2003-212663 Article · December 2003

[20]. Kumar A, and Rangavittal H.K. “Convergence Studies in the Finite Element Analysis of CFRP Shaft under Torsion Using Shell281, Shell181, and Comparison with Analytical Results.” In: Li C., Chandrasekhar U., Onwubolu G. (eds) Advances in Engineering Design and Simulation, (2020), Lecture Notes on Multidisciplinary Industrial Engineering. Springer, Singapore. https://doi.org/10.1007/978-981-13-8468-4_17.

[21]. Knops M. “Analysis of failure in fiber polymer laminates; the theory of Alfred Puck” © 2008 Springer-Verlag Berlin Heidelberg New York.